

# A direct measurement of the relativistic expansion velocity of gamma-ray burst fireballs

E. Molinari<sup>1\*</sup>, S.D. Vergani<sup>2,3</sup>, D. Malesani<sup>4,5</sup>, S. Covino<sup>1</sup>,  
P. D'Avanzo<sup>6,1</sup>, G. Chincarini<sup>7,1</sup>, F.M. Zerbi<sup>1</sup>, L.A. Antonelli<sup>8</sup>,  
P. Conconi<sup>1</sup>, V. Testa<sup>8</sup>, G. Tosti<sup>9</sup>, F. Vitali<sup>8</sup>,  
F. D'Alessio<sup>8</sup>, G. Malaspina<sup>1</sup>, L. Nicastro<sup>10</sup>, E. Palazzi<sup>10</sup>,  
D. Guetta<sup>8</sup>, S. Campana<sup>1</sup>, P. Goldoni<sup>11,12</sup>, N. Masetti<sup>10</sup>,  
E.J.A. Meurs<sup>2</sup>, A. Monfardini<sup>13</sup>, L. Norci<sup>3</sup>, E. Pian<sup>14</sup>,  
S. Piranomonte<sup>8</sup>, D. Rizzuto<sup>1,7</sup>, M. Stefanon<sup>15</sup>, L. Stella<sup>8</sup>,  
G. Tagliaferri<sup>1</sup>, P.A. Ward<sup>2</sup>, G. Ihle<sup>15</sup>, L. Gonzalez<sup>15</sup>,  
A. Pizarro<sup>15</sup>, P. Sinclair<sup>15</sup>, J. Valenzuela<sup>15</sup>

\*To whom correspondence should be addressed. E-mail: emilio.molinari@brera.inaf.it.

1. INAF - Osservatorio Astronomico di Brera, via E. Bianchi 46, I-23807 Merate (LC), Italy.
2. Dunsink Observatory - DIAS, Dunsink lane, Dublin 15, Ireland.
3. School of Physical Sciences and NCPST, Dublin City University - Dublin 9, Ireland.
4. International School for Advanced Studies (SISSA/ISAS), via Beirut 2-4, I-34014 Trieste, Italy.
5. Dark Cosmology Centre, Niels Bohr Institute, University of Copenhagen, Juliane Maries vej 30, DK-2100 København, Denmark.
6. Dipartimento di Fisica e Matematica, Università dell'Insubria, via Valleggio 11, I-22100 Como, Italy.
7. Università degli Studi di Milano Bicocca, piazza delle Scienze 3, I-20126 Milano, Italy.
8. INAF - Osservatorio Astronomico di Roma, via di Frascati 33, I-00040 Monteporzio Catone (Roma), Italy.
9. Dipartimento di Fisica e Osservatorio Astronomico, Università di Perugia, via A. Pascoli, I-06123 Perugia, Italy.
10. INAF-IASF di Bologna, via P. Gobetti 101, I-40129 Bologna, Italy.
11. APC, Laboratoire Astroparticule et Cosmologie, UMR 7164, 11 Place Marcelin Berthelot, F-75231 Paris Cedex 05, France.

12. CEA Saclay, DSM/DAPNIA/Service d'Astrophysique, F-91191, Gif-sûr-Yvette, France.
13. CNRS-CRTBT Centre de Recherches sur les Très Basses Températures, 25 Avenue des Martyrs - BP 166, F-38042 Grenoble, France.
14. INAF - Osservatorio Astronomico di Trieste, via G.B. Tiepolo 11, I-34143 Trieste, Italy.
15. European Southern Observatory, Alonso de Córdova 3107, Vitacura, Casilla 19001, Santiago 19, Chile.

**Gamma-ray bursts are among the most powerful and remote events in the universe. It is commonly thought that these explosions originate inside fireballs expanding ultra-relativistically. Here we report a direct measurement of the relativistic expansion velocity of the fireball. Using the robotic telescope REM located in Chile we were able to catch the infrared afterglow of two gamma-ray bursts before the early maximum. By measuring the delay between the burst onset and the peak of the afterglow light curve, we determine the fireball initial Lorentz factor to be about 400, corresponding to a velocity  $> 99.999\%$  of the light speed.**

Gamma-ray bursts (GRBs) are powerful explosions coming from the remote universe. Their brief prompt emission at soft gamma-ray energies is followed by a fading afterglow of lower energy radiation (radio to X-ray wavelengths) which can be observed for up to weeks or months. The extremely large energies released by GRBs, coupled with their non-thermal photon spectra and short variability timescales, imply that the source of the emission, the so-called fireball, is expanding at relativistic speeds ( $1-3$ ). In the fireball model it is envisaged that the prompt GRB emission is produced inside the fireball itself, while the afterglow is generated when the fireball slows down by impacting the surrounding medium ( $4, 5$ ). Here we present fast-response robotic observations of the near-infrared (NIR) afterglow of the gamma-ray bursts GRB 060418 and GRB 060607A. We are able to clearly detect the afterglow peak and to measure its delay with respect to the prompt emission, thus obtaining for the first time a direct measurement of the initial fireball Lorentz factor  $\Gamma_0$ .

In order to reproduce the observed phenomenology, most of the GRB scenarios proposed and discussed over the years rely on the fireball model (2, 3). A central engine suddenly releases a very large amount of energy which escapes the system as a fireball expanding at relativistic speeds, composed by photons and electron-positron pairs with a small baryonic load. A fraction of the energy is emitted during the prompt event in gamma-rays. The very short time variability implies that this emission takes place at relatively short distances ( $\sim 10^{14}$ – $10^{15}$  cm) from the explosion site. The onset of the afterglow is believed to occur at larger radii ( $\sim 10^{16}$ – $10^{17}$  cm) when the fireball starts decelerating due to the interaction with the surrounding material. During this so-called external shock process, part of the fireball kinetic energy is dissipated into internal energy and can be radiated. The resulting afterglow emission is non-thermal and spans a wide range of wavelengths. According to the standard theory, the afterglow reaches its maximum luminosity when the Lorentz factor has dropped to about half of its initial value, therefore the very early afterglow carries crucial information on the dynamics of the fireball itself (2, 3).

In principle, the afterglow peak should be observed at all frequencies. The detection of this feature in the X-ray region is however difficult. In fact, at these wavelengths the emission can be easily dominated by long-lasting activity from the central engine. The prompt emission tail is usually dominant during the first few hundred seconds (6), and powerful flares (7), likely of internal origin (8), are often observed superimposed on the light curve decay. The afterglow peak has proven difficult to identify also at infrared, optical and ultraviolet frequencies, despite a growing number of early-stage observations. Also at these wavelengths, in fact, the presence of other components, like the optical flash (as in GRB 990123; 9), or the reverberation of the prompt emission radiation (as in GRB 041219A and GRB 050820A; 10, 11), can mask the rise, peak and very early decay of the underlying afterglow. In other cases, as for GRB 030418, the lack of a measured redshift prevented deriving firm conclusions (12).

GRB 060418 (13) and GRB 060607A (14) were detected by the *Swift* satellite (15). Their

prompt gamma-ray emission lasted for about 50 and 100 s, respectively, displaying complex, multi-peaked light curves. They are at redshifts  $z = 1.489$  (16) and  $z = 3.082$  (17) and their isotropic-equivalent energy released in gamma-rays is  $E_\gamma = 9 \times 10^{52}$  and  $\sim 10^{53}$  erg (18, 19). Within 78 and 65 s, respectively, *Swift* slewed to these targets to monitor them at X-ray and optical/ultraviolet wavelengths with the XRT and UVOT instruments. In both cases, the robotic Rapid Eye Mount (REM) telescope (20) also reacted promptly, beginning the observation 64 and 59 s after the triggers (i.e. 39 and 41 s after the reception of the satellite alert).

Figure 1 shows the NIR light curves of the two afterglows. Both present an initial sharp rise, peaking at 100–200 s after the burst. The NIR flux of GRB 060418 decays afterwards as a regular power law. The NIR light curve of GRB 060607A shows a similar, smooth behaviour up to  $\sim 1000$  s after the trigger, followed by a rebrightening lasting  $\sim 2000$  s. To quantitatively evaluate the peak time, we fitted the NIR light curves by using a smoothly broken power-law (21) (any other suitable functional forms provides comparable results; see Fig. 1 and Table 1), obtaining peak times of  $153 \pm 10$  and  $180 \pm 6$  s ( $1\sigma$  error) for GRB 060418 and GRB 060607A, respectively.

As for many other GRBs observed by *Swift* (22), the early X-ray light curves of both events show several, intense flares superimposed on the power-law decay. In particular, for GRB 060418 a bright flare is active between  $\sim 115$  and 185 s. The X-ray light curve of GRB 060607A is more complex and presents two large flares within the first 400 s. After that the flux density decreases with a shallow power law (with small-scale variability) until steepening sharply at  $t \sim 10^4$  s.

By comparing the X-ray and NIR light curves of both bursts, it is apparent that the flaring activity, if any, is much weaker at NIR wavelengths. It is thus likely that the afterglow peak, visible in the NIR, is hidden in the X-ray region. In the case of GRB 060418, thanks to our multicolour data, this can be confirmed by considering the NIR/X-ray spectral energy distribu-

tion. The extrapolation of the NIR flux to the X-ray band predicts at the time of the afterglow peak a flux much lower than observed, implying that another component is powering the X-ray emission. After a few hundred seconds, where no flares are present, this is not the case anymore, and we can easily model the spectrum from the NIR to the X-rays by using the standard afterglow theory. In particular, the spectral and decay indices of GRB 060418 at NIR and X-ray frequencies are remarkably consistent with the behaviour predicted for a fireball expanding in a homogeneous ambient. For GRB 060607A, the light curve is complicated by several flares, and we lack multicolour data, so that a detailed analysis is not possible. Its behaviour is nevertheless broadly consistent with a homogeneous ambient as well.

For both bursts the peak time  $t_{\text{peak}}$  is longer than the burst duration. In this case the detection of the afterglow peak yields a direct measurement of the fireball Lorentz factor at the afterglow onset (3, 23)  $\Gamma(t_{\text{peak}}) = 1/\sqrt{1 - v^2/c^2}$  (where  $v$  and  $c$  are the speed of the fireball and of the light, respectively):

$$\Gamma(t_{\text{peak}}) = \left[ \frac{3E_\gamma(1+z)^3}{32\pi n m_p c^5 \eta t_{\text{peak}}^3} \right]^{1/8} \sim 160 \left[ \frac{E_{\gamma,53}(1+z)^3}{\eta_{0.2} n_0 t_{\text{peak},2}^3} \right]^{1/8}, \quad (1)$$

where  $E_\gamma = 10^{53} E_{\gamma,53}$  erg is the isotropic-equivalent energy released by the GRB in gamma-rays,  $n = n_0 \text{ cm}^{-3}$  is the circumburst particle number density,  $m_p$  is the proton mass,  $t_{\text{peak}} = 100 t_{\text{peak},2}$  s is the peak time in the observer frame, and  $\eta = 0.2 \eta_{0.2}$  is the radiative efficiency. Since the fireball initial Lorentz factor is  $\Gamma_0 \approx 2\Gamma(t_{\text{peak}})$  (3), substituting the measured quantities and normalizing to the typical values  $n = 1 \text{ cm}^{-3}$  and  $\eta = 0.2$  (24), we infer for both bursts  $\Gamma_0 \approx 400 (\eta_{0.2} n_0)^{-1/8}$ . This value is very weakly dependent on the unknown parameters  $n$  and  $\eta$ , and therefore provides a robust determination of  $\Gamma_0$ .

This is the first time that  $\Gamma_0$  is directly measured from the observations of a GRB. Such a value is well within the range  $50 \lesssim \Gamma_0 \lesssim 1000$  envisaged by the standard fireball model (2, 3, 25). It is also in agreement with existing measured lower limits (26, 8). The determination of

$t_{\text{peak}}$  is in principle affected by the choice of the time origin  $t_0$  (27, 28) (we have set  $t_0$  to the BAT trigger time). It has been shown, however, that this effect is small (28), and mostly affects the rise and decay slopes rather than the peak time (especially given that  $t_{\text{peak}}$  is larger than the burst duration for GRB 060418 and GRB 060607A). The measurement of  $\Gamma_0$  is thus not very sensitive to the exact choice of  $t_0$ .

Having measured the Lorentz factor, we can also derive other fundamental quantities characterizing the fireball. In particular, the deceleration radius is  $R_{\text{dec}} \approx 2ct_{\text{peak}}[\Gamma(t_{\text{peak}})]^2/(1+z) \approx 10^{17}$  cm. This is much larger than the scale of  $10^{15}$  cm where the internal shocks are believed to power the prompt emission (4), thus providing further evidence for a different origin for the prompt and afterglow stages of the GRB. We can also compute the isotropic-equivalent baryonic load of the fireball  $M_{\text{fb}} = E/(\Gamma_0 c^2) \approx 7 \times 10^{-4} M_{\odot}$ , where  $M_{\odot}$  is the mass of the Sun and  $E = E_{\gamma}/\eta$ .

For both bursts, we could not detect any reverse shock emission. The lack of such flashes has already been noticed previously (29). Among the many possible mechanisms to explain the lack of this component, strong suppression (or even total lack) of reverse shock emission is naturally expected if the outflow is Poynting-flux dominated (30).

The very fast response REM observations presented here provide crucial information on the GRB fireball parameters, most importantly its initial Lorentz factor. These are a key to constrain the properties of the still mysterious GRB engine, including the production and acceleration of the jet, and the release of the electromagnetic energy.

## References and Notes

1. E. E. Fenimore, R. I. Epstein, C. Ho, *Astrophys. J.* **97**, 59 (1993).
2. T. Piran, *Phys. Rep.* **333**, 529 (2000).
3. P. Mészáros, *Rep. on Progr. in Phys.* **69**, 2259 (2006).

4. M. J. Rees, P. Mészáros, *Astrophys. J* **430**, 93 (1994).
5. P. Mészáros, M. J. Rees, *Astrophys. J* **476**, 232 (1994).
6. G. Tagliaferri *et al.*, *Nature* **436**, 985 (2005).
7. D. N. Burrows *et al.*, *Science* **309**, 1833 (2005).
8. B. Zhang *et al.*, *Astrophys. J.* **642**, 354 (2006).
9. C. Akerlof *et al.*, *Nature* **398**, 400 (1999).
10. W. T. Vestrand *et al.*, *Nature* **435**, 178 (2005).
11. W. T. Vestrand *et al.*, *Nature* **442**, 172 (2006).
12. E. S. Rykoff *et al.*, *Astrophys. J.* **601**, 1013 (2004).
13. A. D. Falcone *et al.*, *GCN Circ.* **4966** (2006).
14. H. Z. Ziaepour *et al.*, *GCN Circ.* **5233** (2006).
15. N. Gehrels *et al.*, *Astrophys. J.* **611**, 1005 (2004).
16. A. K. Dupree, E. Falco, J. X. Prochaska, H.-W. Chen, J. S. Bloom, *GCN Circ.* **4969** (2006).
17. C. Ledoux, P. Vreeswijk, A. Smette, A. Jaunsen, A. Kaufer, *GCN Circ.* **5237** (2006).
18. S. Golenetskii *et al.*, *GCN Circ.* **4989** (2006).
19. J. Tueller *et al.*, *GCN Circ.* **5242** (2006).
20. F. M. Zerbi *et al.*, *Astron. Nach.* **322**, 275 (2001).
21. K. Beuermann *et al.*, *Astron. Astrophys.* **352**, L26 (1999).
22. G. Chincarini, in *Frontier Objects in Astrophysics and Particle Physics*, F. Giovannelli, G. Mannocchi, Eds. (Editrice Compositori, Bologna, 2007), in press.

23. R. Sari, T. Piran, *Astrophys. J.* **520**, 641 (1999).
  24. J. S. Bloom, D. A. Frail, S. R. Kulkarni, *Astrophys. J.* **594**, 674 (2003).
  25. D. Guetta, M. Spada, E. Waxman, *Astrophys. J.* **557**, 399 (2001).
  26. Y. Lithwick, R. Sari, *Astrophys. J.* **555**, 540 (2001).
  27. D. Lazzati, M. C. Begelman, *Astrophys. J.* **641**, 972 (2006).
  28. R. Quimby *et al.*, *Astrophys. J.* **640**, 402 (2006).
  29. P. W. A. Roming *et al.*, *Astrophys. J.* **652**, 1416 (2006).
  30. B. Zhang, S. Kobayashi, *Astrophys. J.* **628**, 315 (2005).
1. The REM project has been accomplished thanks to the support of the Italian Ministry of Education (MURST - COFIN, P.I. G.C.). In addition, part of the instrumentation has been partially supported by ASI (ROSS spectrograph, PI E.P.), by CNAA and by the *Swift* Project (supported by ASI) while present maintenance and operation of the REM telescope is supported by INAF (PI E.M.). We also acknowledge the sponsorship of the Italian division of AMD who provided computers for the REM observatory. REM is the result of a collaboration between a group of Italian research institutes, coordinated by the Osservatorio Astronomico di Brera, the Laboratoire Astroparticule et Cosmologie and the DSM/DAPNIA/Service d'Astrophysique (France), the Dunsink Observatory and UCD (Ireland). S.D.V. and D.M. are supported by SFI and IDA, respectively. We thank Massimo Della Valle and D. Alexander Kann for discussion. Browse the REM home page at <http://www.rem.inaf.it>.



**Table 1.** Best fit values to the light curves of GRB 060418 and GRB 060607A ( $1\sigma$  errors). For the latter we used only data for  $t < 1000$  s. We adopt the functional form  $F(t) = F_0 / [(t/t_b)^{\kappa\alpha_r} + (t/t_b)^{\kappa\alpha_d}]^{1/\kappa}$  (21), where  $F_0$  is a normalization constant,  $\alpha_{r(d)}$  is the slope of the rise (decay) phase and  $\kappa$  is a smoothness parameter. The time  $t_{\text{peak}}$  at which the curve reaches its maximum is related to  $t_b$  according to  $t_{\text{peak}} = t_b(-\alpha_r/\alpha_d)^{1/[\kappa(\alpha_d-\alpha_r)]}$ . The relatively large  $\chi^2$  of the fit results from small-scale irregularities present throughout the light curve (see Figs. 1 and 2).

GRB	$t_{\text{peak}}$ (s)	$t_b$ (s)	$\alpha_r$	$\alpha_d$	$\kappa$	$\chi^2/\text{d.o.f.}$
060418	$153^{+10}_{-10}$	$127^{+18}_{-21}$	$-2.7^{+1.0}_{-1.7}$	$1.28^{+0.05}_{-0.05}$	$1.0^{+0.4}_{-0.4}$	33.3/16
060607A	$180^{+5}_{-6}$	$153^{+12}_{-12}$	$-3.6^{+0.8}_{-1.1}$	$1.27^{+0.16}_{-0.11}$	$1.3^{+0.9}_{-1.1}$	28.5/19

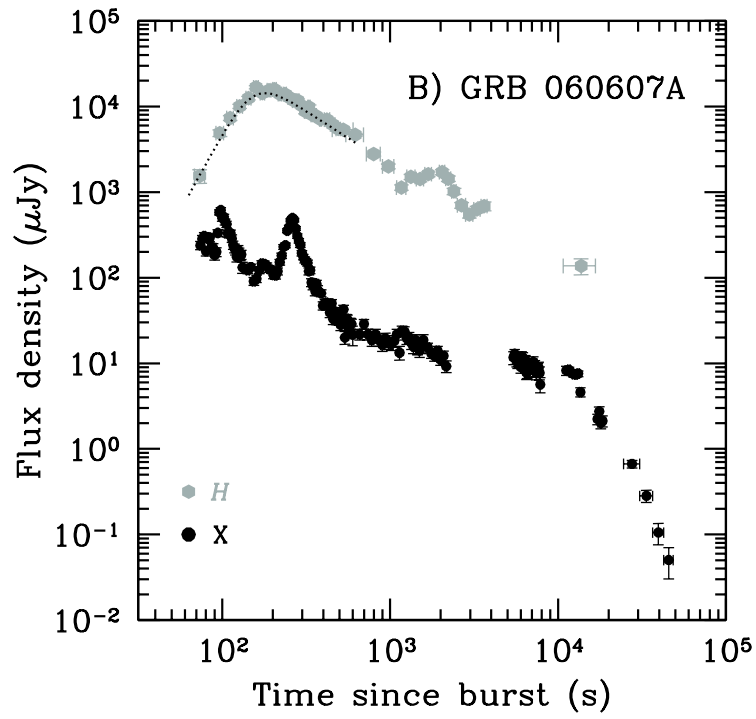
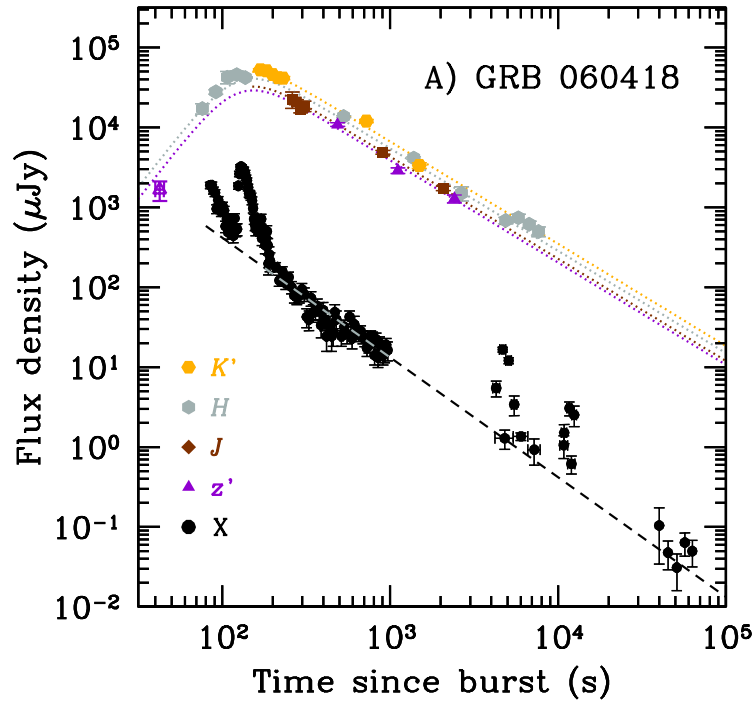


**Fig. 1.** Near-infrared light curves of the afterglows of GRB 060418 (A) and GRB 060607A (B). The dotted lines show the best fits using the smoothly broken power law (Table 1). The photometric values are reported in Tables S1 and S2. GRB 060418 was observed cycling through the  $z'JHK'$  filters, in order to obtain also spectral information. The evolution is consistent with being achromatic. The decay slope of the X-ray afterglow (excluding flares, dashed line) is  $\alpha_X = 1.50 \pm 0.06$ , while the spectral index in the interval 200–1000 s is  $\beta_X = 1.30 \pm 0.05$ . This afterglow is thus perfectly consistent with a homogeneous environment, for which  $\alpha_X = 3\beta_X/2 - 1/2$  and  $\alpha_{\text{opt}} = \alpha_X - 1/4$  is predicted. GRB 060607A observations were performed only in the  $H$  band in order to get a denser sampling of the light curve. REM is a 60 cm diameter fast-reacting ( $10 \text{ deg s}^{-1}$  pointing speed) telescope located at the Cerro La Silla premises of the European Southern Observatory, Chile. The telescope hosts REMIR, an infrared imaging camera, and ROSS, an optical imager and slitless spectrograph. The two cameras observe simultaneously the same field of view of  $10' \times 10'$  thanks to a dichroic. REMIR operates in the range 1.0–2.3  $\mu\text{m}$  ( $z'JHK'$ ), reaching a limiting magnitude  $H = 15.5$  in a 5 s exposure ( $S/N = 3$ ). In the same time ROSS reaches  $R = 16.0$  ( $S/N = 3$ ). ROSS could not observe these two GRBs due to maintenance work.

## **Supporting Online Tables**

Table 1: Observation log for GRB 060418. The time  $t_0$  indicates the BAT trigger time, 2006 April 18.12926 UT. We report the mean time of observation in column 1, the time delay between the GRB trigger and the observation in column 2, the exposure time in column 3, the adopted filter in column 4, and the observed magnitude with its error ( $1\sigma$ ) in column 5.

\* M. Nysewander *et al.*, *GCN Circ.* **4971** (2006).

Mean time (UT)	$t - t_0$ (s)	Exp. time (s)	Filter	Magnitude
Apr 18.12974	40	5	$z$	$15.3 \pm 0.3^*$
Apr 18.13371	479	100	$z'$	$13.26 \pm 0.06$
Apr 18.14215	1114	100	$z'$	$14.70 \pm 0.09$
Apr 18.15722	2416	100	$z'$	$15.58 \pm 0.12$
Apr 18.13264	292	100	$J$	$12.33 \pm 0.05$
Apr 18.13975	906	150	$J$	$13.82 \pm 0.06$
Apr 18.15323	2071	300	$J$	$14.94 \pm 0.07$
Apr 18.13014	76	10	$H$	$11.98 \pm 0.16$
Apr 18.13032	92	10	$H$	$11.46 \pm 0.07$
Apr 18.13050	107	10	$H$	$11.00 \pm 0.19$
Apr 18.13067	122	10	$H$	$10.92 \pm 0.12$
Apr 18.13085	137	10	$H$	$11.01 \pm 0.02$
Apr 18.13538	529	150	$H$	$12.24 \pm 0.03$
Apr 18.14527	1383	150	$H$	$13.57 \pm 0.04$
Apr 18.16008	2663	150	$H$	$14.89 \pm 0.22$
Apr 18.18578	4883	150	$H$	$15.48 \pm 0.10$
Apr 18.19649	5809	150	$H$	$15.40 \pm 0.12$
Apr 18.20720	6734	150	$H$	$15.60 \pm 0.10$
Apr 18.21791	7659	150	$H$	$15.83 \pm 0.15$
Apr 18.13121	168	10	$K'$	$10.23 \pm 0.04$
Apr 18.13139	184	10	$K'$	$10.26 \pm 0.03$
Apr 18.13157	200	10	$K'$	$10.38 \pm 0.03$
Apr 18.13175	215	10	$K'$	$10.48 \pm 0.05$
Apr 18.13192	230	10	$K'$	$10.49 \pm 0.05$
Apr 18.14652	1491	300	$K'$	$13.14 \pm 0.09$

Table 2: Observation log for GRB 060607A. The time  $t_0$  indicates the BAT trigger time, 2006 June 7.21682 UT. We report the mean time of observation in column 1, the time delay between the GRB trigger and the observation in column 2, the exposure time in column 3, the adopted filter in column 4, and the observed magnitude with its error ( $1\sigma$ ) in column 5.

Mean time (UT)	$t - t_0$ (s)	Exp. time (s)	Filter	Magnitude
Jun 7.21767	73	10	<i>H</i>	$14.60 \pm 0.20$
Jun 7.21794	97	10	<i>H</i>	$13.35 \pm 0.10$
Jun 7.21811	111	10	<i>H</i>	$12.91 \pm 0.07$
Jun 7.21829	127	10	<i>H</i>	$12.57 \pm 0.06$
Jun 7.21848	143	10	<i>H</i>	$12.33 \pm 0.05$
Jun 7.21866	159	10	<i>H</i>	$12.01 \pm 0.05$
Jun 7.21883	174	10	<i>H</i>	$12.18 \pm 0.05$
Jun 7.21902	190	10	<i>H</i>	$12.10 \pm 0.05$
Jun 7.21919	205	10	<i>H</i>	$12.07 \pm 0.05$
Jun 7.21937	220	10	<i>H</i>	$12.21 \pm 0.05$
Jun 7.21955	236	10	<i>H</i>	$12.21 \pm 0.05$
Jun 7.21973	251	10	<i>H</i>	$12.31 \pm 0.05$
Jun 7.21991	267	10	<i>H</i>	$12.40 \pm 0.05$
Jun 7.22008	282	10	<i>H</i>	$12.40 \pm 0.05$
Jun 7.22027	298	10	<i>H</i>	$12.55 \pm 0.06$
Jun 7.22045	314	10	<i>H</i>	$12.72 \pm 0.06$
Jun 7.22062	328	10	<i>H</i>	$12.59 \pm 0.06$
Jun 7.22080	344	10	<i>H</i>	$12.82 \pm 0.07$
Jun 7.22098	359	10	<i>H</i>	$12.84 \pm 0.07$
Jun 7.22128	385	30	<i>H</i>	$12.95 \pm 0.05$
Jun 7.22169	421	30	<i>H</i>	$12.96 \pm 0.05$
Jun 7.22209	455	30	<i>H</i>	$13.10 \pm 0.05$
Jun 7.22251	492	30	<i>H</i>	$13.23 \pm 0.05$
Jun 7.22292	527	30	<i>H</i>	$13.25 \pm 0.05$
Jun 7.22400	620	150	<i>H</i>	$13.40 \pm 0.04$
Jun 7.22606	798	150	<i>H</i>	$13.96 \pm 0.06$
Jun 7.22812	976	150	<i>H</i>	$14.32 \pm 0.07$
Jun 7.23033	1167	150	<i>H</i>	$14.94 \pm 0.08$
Jun 7.23223	1331	150	<i>H</i>	$14.63 \pm 0.07$
Jun 7.23427	1508	150	<i>H</i>	$14.69 \pm 0.08$
Jun 7.23635	1687	150	<i>H</i>	$14.55 \pm 0.07$
Jun 7.24047	2043	150	<i>H</i>	$14.49 \pm 0.07$
Jun 7.24253	2221	150	<i>H</i>	$14.68 \pm 0.08$
Jun 7.24459	2399	150	<i>H</i>	$15.05 \pm 0.09$
Jun 7.24767	2665	300	<i>H</i>	$15.46 \pm 0.08$
Jun 7.25113	2964	300	<i>H</i>	$15.73 \pm 0.10$
Jun 7.25493	3293	300	<i>H</i>	$15.58 \pm 0.09$
Jun 7.25886	3632	150	<i>H</i>	$15.48 \pm 0.13$
Jun 7.37574	13730	6000	<i>H</i>	$17.23 \pm 0.23$